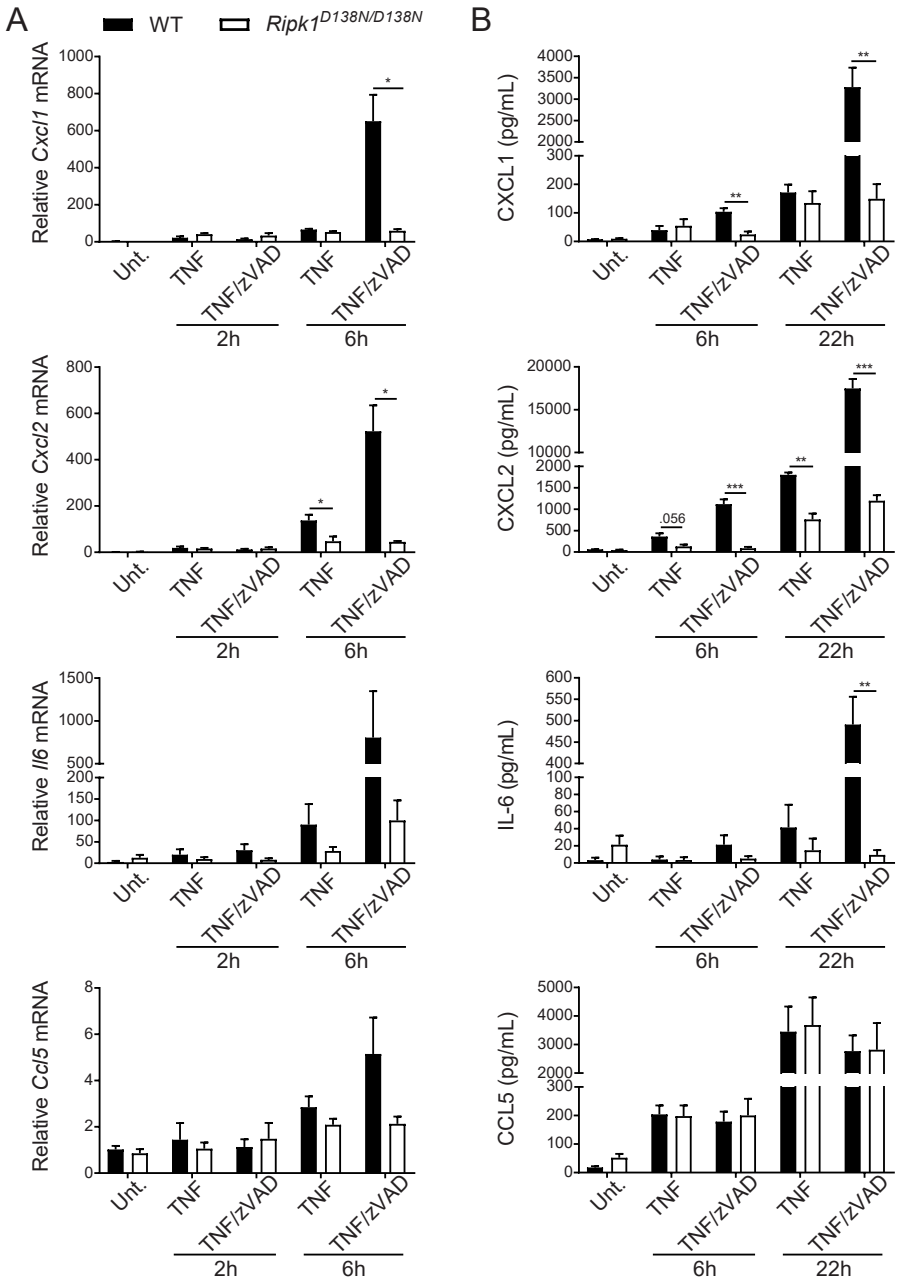

Supplementary Figure 1. RIPK1 kinase activity contributes to TNF- and TNF/zVAD-induced chemokine production in vitro. (A) Quantitative RT-PCR analysis of *Cxcl1*, *Cxcl2*, *Il6*, and *Ccl5* expression in WT and *Ripk1*$^{D138N/D138N}$ primary macrophages treated with TNF or TNF/zVAD for 2 or 6 hours (n = 3 mice). Graphs show relative mRNA expression normalized to *Actin*. (B) Secretion of CXCL1, CXCL2, IL-6 and CCL5 as determined by ELISA in WT and *Ripk1*$^{D138N/D138N}$ primary macrophages 6 or 22 hours after addition of TNF or TNF/zVAD (n = 3 mice). Error bars represent mean ± SEM. *p<0.05, **p<0.01, ***p<0.001, by 2-tailed Student's *t* test.

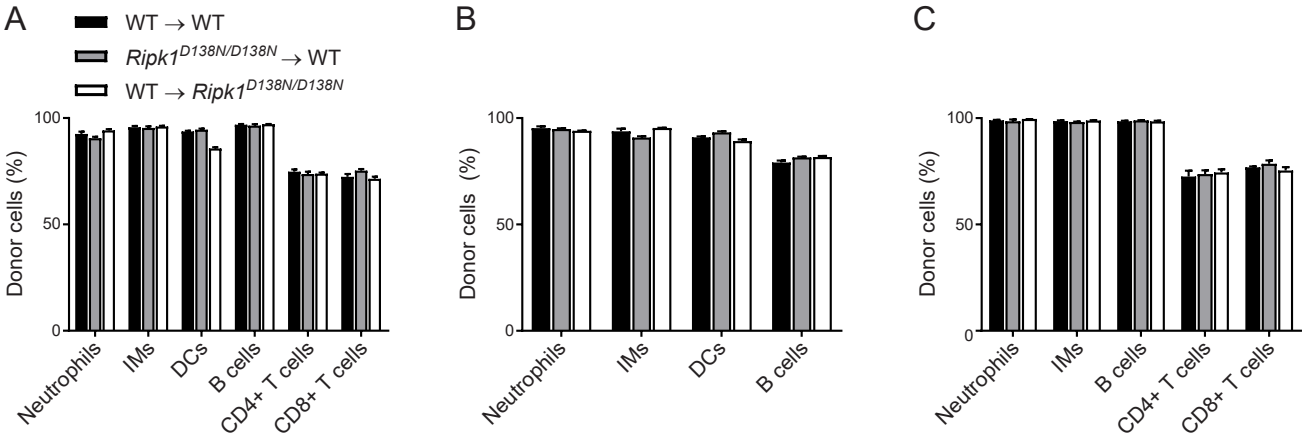

Supplementary Figure 2. Kinase inactive RIPK1 bone marrow cells effectively repopulate lethally irradiated hosts. Graphs depicting the percentage of donor-derived myeloid and lymphoid lineages in the spleen (A), bone marrow (B), and blood (C) at 8 weeks post-transplantation (n = 4-8 mice). Error bars represent mean ± SEM. IMs: Inflammatory Macrophages, DCs: Dendritic Cells.

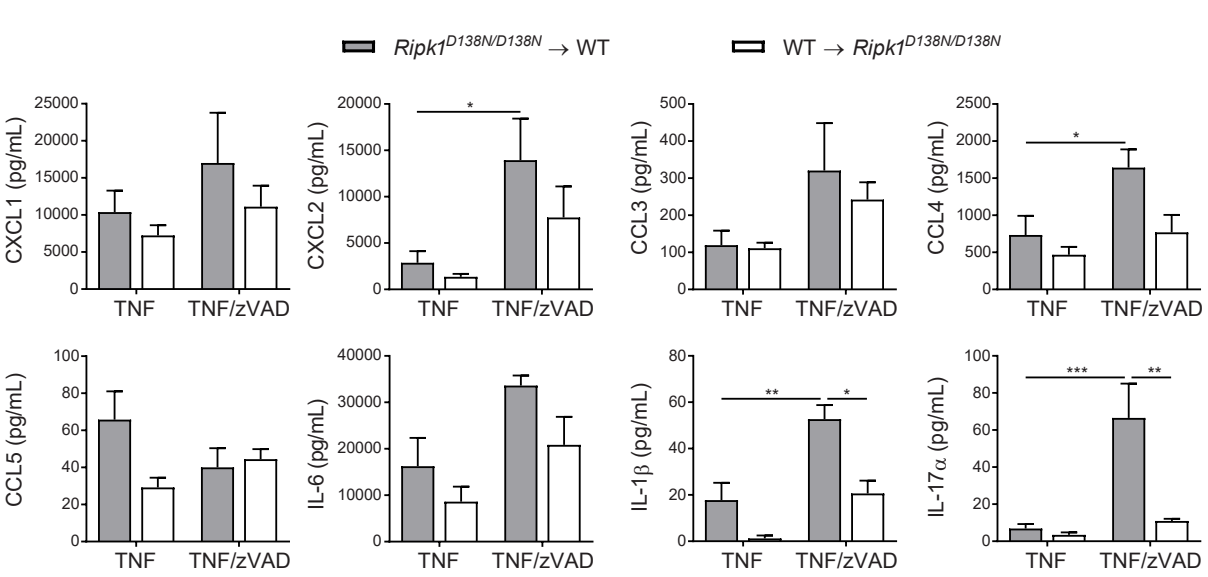

Supplementary Figure 3. Reduced cytokine and chemokine production in TNF/zVAD-treated RIPK1 kinase inactive hosts. Plasma cytokine and chemokine levels in reconstituted mice 2 hours after intravenous TNF or TNF/zVAD administration (n = 3-7). TNF-induced levels are repeated from Figure 4A. Error bars represent mean ± SEM. *p<0.05, **p<0.01, ***p<0.001, by two-way ANOVA with post hoc Tukey test.

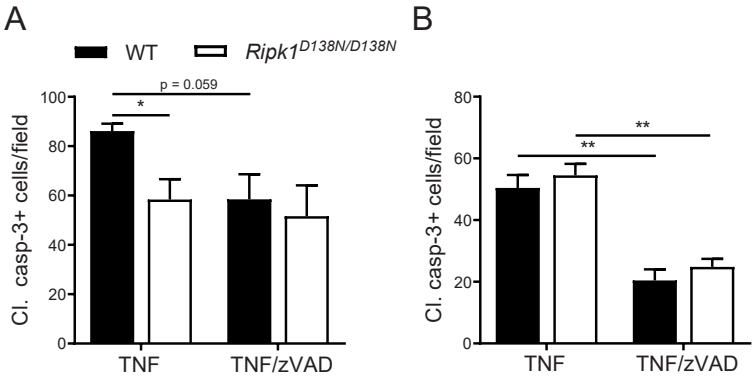

Supplementary Figure 4. Kinase inactive RIPK1 mice are modestly protected from TNF-induced ileal but not colonic intestinal epithelial apoptosis. Quantification of cleaved caspase-3 positive cells per 40x field in the ileum (A) and colon (B) of WT and *Ripk1*$^{D138N/D138N}$ mice 2 hours after TNF or TNF-zVAD administration (n = 3). Error bars represent mean ± SEM. *p<0.05, **p<0.01, by 2-tailed Student's *t* test.

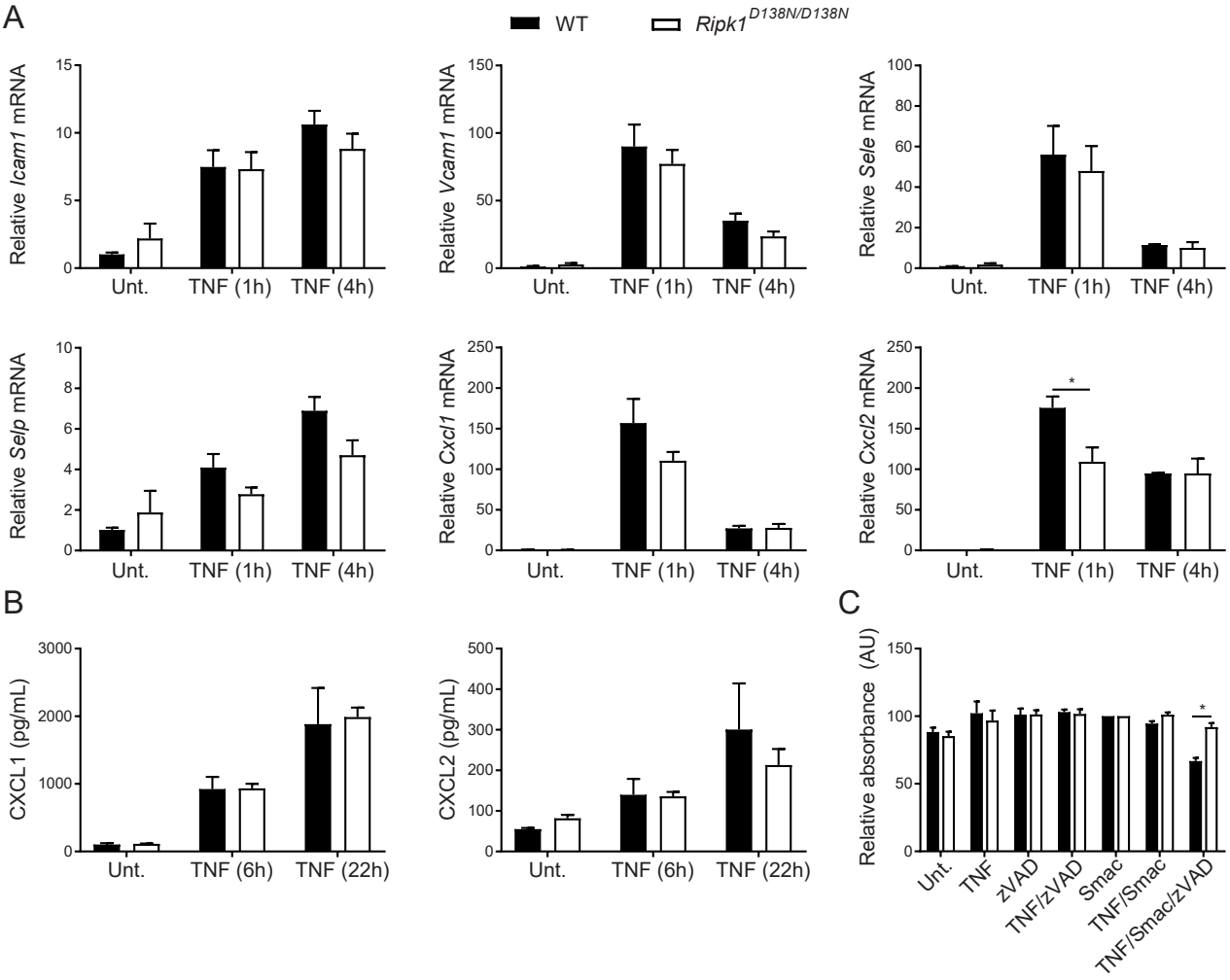

Supplementary Figure 5. RIPK1 kinase activity is required for lung endothelial necroptosis induced by TNF/Smac/zVAD treatment but not for upregulation of adhesion molecules in endothelial cells in vitro. (A) Relative expression of *Icam1*, *Vcam1*, *Sele*, *Selp*, *Cxcl1* and *Cxcl2* in WT and *Ripk1*$^{D138N/D138N}$ primary lung endothelial cells treated with TNF for 1 or 4 hours (n = 3-4 mice). Graphs show relative mRNA expression normalized to *Actin*. (B) Secretion of CXCL1 and CXCL2 in WT and *Ripk1*$^{D138N/D138N}$ primary lung endothelial cells 6 or 22 hours after addition of TNF (n = 3-4 mice). (C) Primary lung endothelial cells isolated from WT and *Ripk1*$^{D138N/D138N}$ mice were treated with TNF (10 ng/ml), zVAD (20 μM), and/or Smac mimetic (1 μM) and cell viability was measured using MTS assay (n = 3 mice). Error bars represent mean ± SEM. *p<0.05, by 2-tailed Student's *t* test.

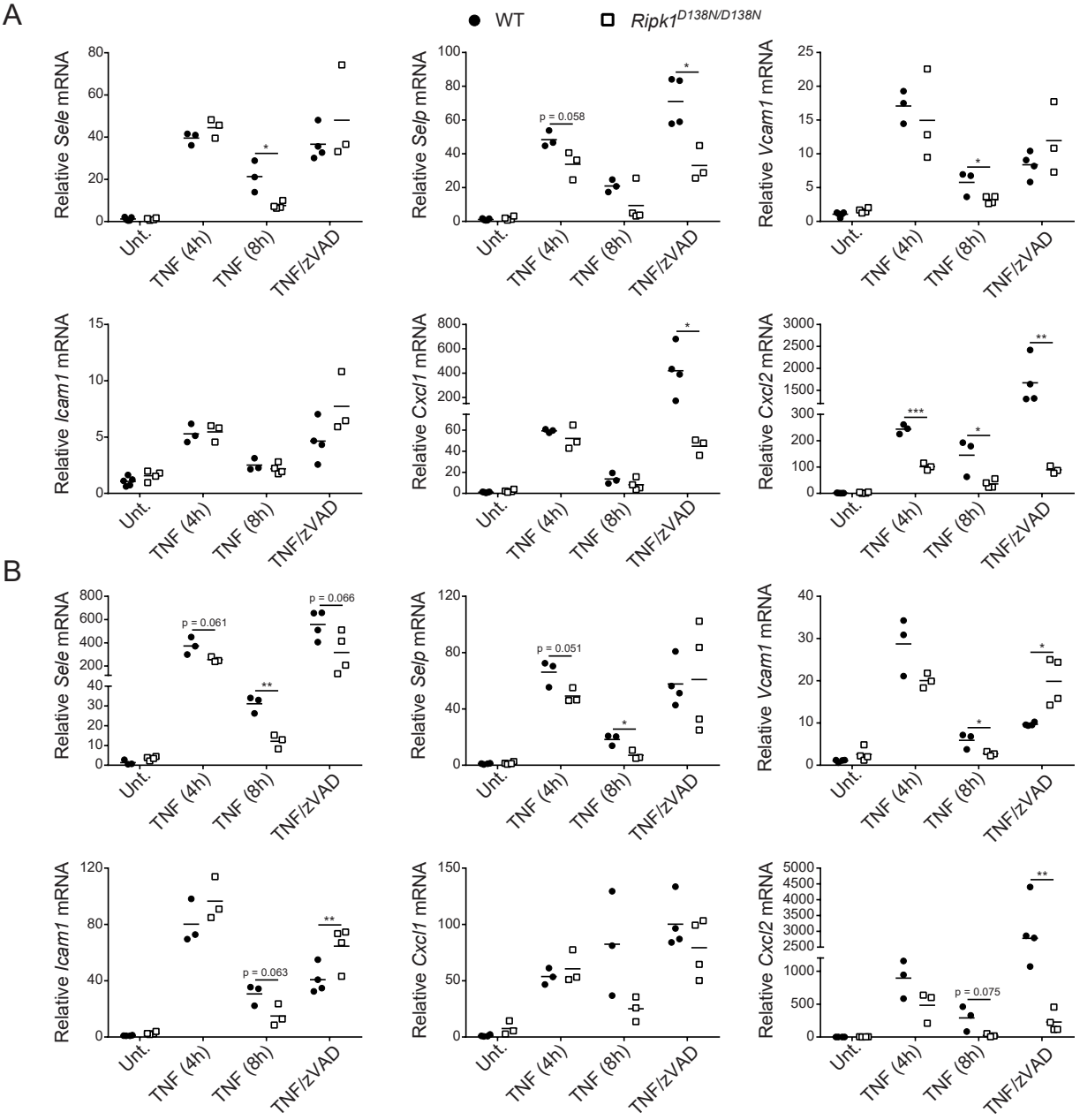

Supplementary Figure 6. Kinase inactive RIPK1 mice upregulate adhesion molecules but exhibit decreased *P-selectin* and *Cxcl2* expression in lung and liver treated with TNF or TNF/zVAD. Relative expression of *Sele*, *Selp*, *Vcam1*, *Icam1*, *Cxcl1* and *Cxcl2* in WT and *Ripk1*$^{D138N/D138N}$ lungs (A) or livers (B) after TNF (4 or 8h) or TNF/zVAD (4h) treatment (n = 3-4 mice). Graphs show relative mRNA expression normalized to *Actin*. *p<0.05, **p<0.01, ***p<0.001, by 2-tailed Student's *t* test.

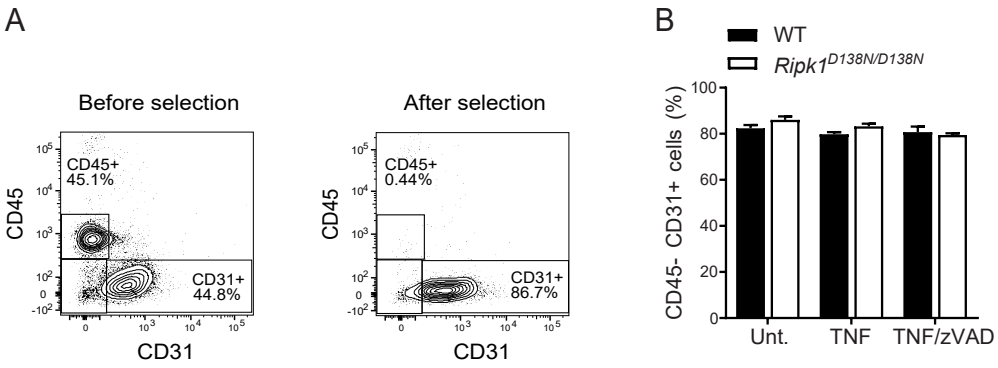

Supplementary Figure 7. Gating strategy and purity of endothelial cells isolated from TNF- or TNF/zVAD-treated WT and *Ripk1*$^{D138N/D138N}$ mice. (A) Gating strategy for the purification of liver endothelial cells using FACS. CD45+ cells were depleted before enriching for CD146+ cells and gating on CD45- CD31+ cells. (B) Quantification of liver endothelial cell enrichment from untreated (Unt.), or TNF- or TNF/zVAD-treated WT and *Ripk1*$^{D138N/D138N}$ mice (n = 3). Error bars represent mean ± SEM.

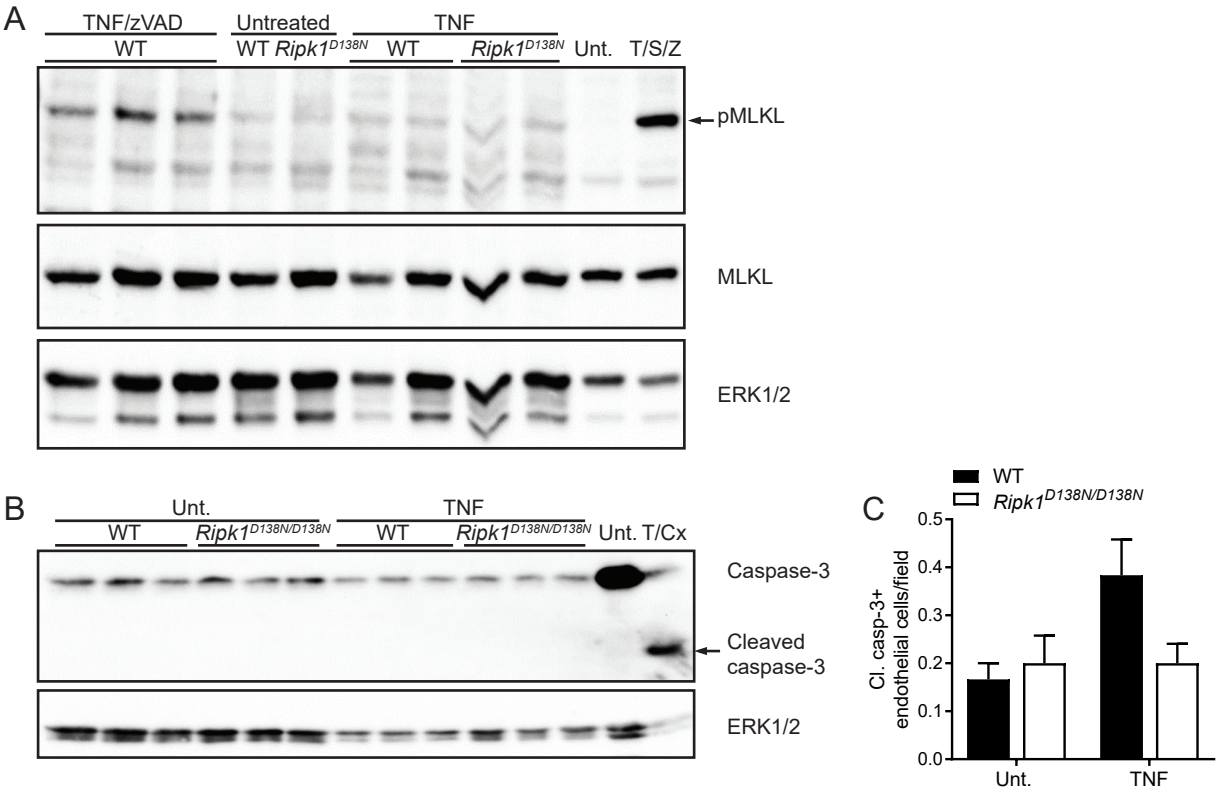

Supplementary Figure 8. pMLKL is detected in liver endothelial cells from TNF/zVAD-treated but not TNF-treated mice. (A) WT and *Ripk1*$^{D138N/D138N}$ endothelial cells were isolated from livers of untreated, TNF-, or TNF/zVAD-treated mice. A representative western blot showing protein lysates probed with antibodies to phospho-MLKL, MLKL, ERK1/2 is depicted. Lysates from murine embryonic fibroblasts (MEF) left untreated (Unt.) or stimulated with TNF, SMAC mimetics, and zVAD-fmk (T/S/Z) served as a positive control. (Lysates were generated and analyzed from 7 WT and 7 *Ripk1*$^{D138N/D138N}$ TNF-treated mice). (B) Lysates from WT or *Ripk1*$^{D138N/D138N}$ liver endothelial cells isolated from untreated or TNF-treated mice were probed with antibodies to full length and cleaved caspase-3 (CC3) or ERK1/2 as a loading control (n = 3 mice). MEFs left untreated (Unt.) or treated with TNF and cycloheximide (T/Cx) served as controls for CC3 detection. (C) Quantification of cleaved caspase-3-positive liver endothelial cells from untreated or TNF-treated WT and *Ripk1*$^{D138N/D138N}$ mice by IHC (n = 3-6 mice per group). Error bars represent mean ± SEM.

Supplementary Table 1. qPCR primers for mouse genes

Gene symbol	Direction	Primer sequence (5' to 3')
Actin	For	CGAGGCCCAGAGCAAGAGAG
	Rev	CGGTTGGCCTTAGGGTTCAG
Sele	For	ATGCCTCGCGCTTTCTCTC
	Rev	GTAGTCCCGCTGACAGTATGC
Selp	For	CATCTGGTTCAGTGCTTTGATCT
	Rev	ACCCGTGAGTTATTCCATGAGT
Icam1	For	GTGATGCTCAGGTATCCATCCA
	Rev	CACAGTTCTCAAAGCACAGCG
Vcam1	For	AGTTGGGGATTCGGTTGTTCT
	Rev	CCCCTCATTCCTTACCACCC
Il6	For	AACGATGATGCACTTGCAGA
	Rev	GAGCATTGGAAATTGGGGTA
Ccl5	For	GCCCACGTCAAGGAGTATTTCTA
	Rev	ACACACTTGGCGGTTCCTTC
Cxcl1	For	CTGGGATTCACCTCAAGAACATC
	Rev	CAGGGTCAAGGCAAGCCTC
Cxcl2	For	CCAACCACCAGGCTACAGG
	Rev	GCGTCACACTCAAGCTCTG

Supplementary Table 2. Flow cytometry antibodies

Antibody	Clone	Fluorophore	Source
CD11b	M1/70	FITC	BioLegend
Gr1	RB6-8C5	PE	BD Biosciences
Ly6C	HK1.4	APC	BioLegend
Cd11c	N418	Pacific Blue	BioLegend
CD45.1	A20	PerCP/Cy5.5	BioLegend
CD45.2	104	PeCy7	BioLegend
CD4	RM4-5	PerCP/Cy5.5	BioLegend
CD8	53-6.7	FITC	BD Biosciences
B220	RA3-6B2	PE	BioLegend
CD45	30-F11	APC-Cy7	BD Biosciences
CD31	390	FITC	BioLegend